Nuclear Physics A376 (1982) 309 324
© North-Holland Publishing Company

TWO-PROTON PICKUP IN THE ZIRCONIUM REGION USING THE (^{6}Li, ^{8}B) REACTION

R. S. TICKLE and W. S. GRAY

Department of Physics, University of Michigan, Ann Arbor, Michigan 48109, USA

and

R. D. BENT †

Indiana University Cyclotron Facility, Bloomington, Indiana 47405, USA

Received 7 September 1981

Abstract: Spectra at $\theta_{lab} = 8°$ have been measured for the ^{92,94,96,98,100}Mo(^{6}Li, ^{8}B)^{90,92,94,96,98}Zr and ^{90,92,94}Zr(^{6}Li, ^{8}B)^{88,90,92}Sr two-proton pickup reactions at 90 MeV. The strongest transitions to levels in the Zr isotopes are the $0^+ \rightarrow 0^+$ transitions to the g.s. and first excited 0^+ states. The salient feature of the five Zr spectra is the large increase in 0_2^+ transition strength relative to that of the g.s. which is observed in the two heaviest isotopes, ^{96,98}Zr. In ^{90}Zr, the 0_2^+ transition is weak whereas it is the dominant transition in ^{98}Zr with twice the g.s. strength. These large variations in relative cross section, which are reproduced by DWBA calculations, are attributed to changing g.s. proton configurations in Zr. In the Sr spectra, which are distinctly different from the Zr spectra, the strongest transitions to excited states are to 2^+ rather than 0^+ states. The (^{6}Li, ^{8}B) reaction seems to be adequately described as a one-step cluster transfer of a $T = 1$, $S = 0$ proton pair. The suitability of this reaction for measurements of two-proton pickup is discussed.

E | NUCLEAR REACTIONS ^{92,94,96,98,100}Mo(^{6}Li, ^{8}B), ^{90,92,94}Zr(^{6}Li, ^{8}B), $E = 90$ MeV; measured $\sigma(E_{^8B}, \theta_{lab} = 8°)$. ^{90}Zr(^{6}Li, ^{8}B)^{88}Sr$_{g.s., 2^+}$; measured $\sigma(\theta)$. Calculated spectroscopic amplitudes, direct transfer cross sections and compared with data. Magnetic spectrometer. Enriched targets.

1. Introduction

It is now well established that reactions which transfer two identical nucleons are valuable spectroscopic tools in characterizing nuclear energy levels. For example, the (t, p) and (p, t) two-neutron stripping and pickup reactions have been used [1]) throughout the periodic table as sensitive probes to study correlations between nuclear wave functions. These reactions have the advantages of relatively large cross sections which are often in the mb range, angular distributions characteristic of the L-transfer, and simplicity of analysis based on the assumption of direct transfer of a $T = 1$, $S = 0$ neutron pair in a relative s-state.

† Work supported in part by the US National Science Foundation.

Unfortunately, at this time there exist no equally suitable reactions for the study of proton pairing correlations and two-proton particle and hole configurations. In two-proton stripping experiments, the most used reaction has been (^{3}He, n). As is well known, this reaction, although relatively simple to analyze, suffers from a substantial experimental disadvantage in that it requires a measurement of neutron energy using time-of-flight techniques with the attendant difficulty of achieving adequate resolution, particularly at the higher energies. Various heavy-ion reactions have been used less frequently [2]) and, depending on the reaction, often exhibit undesirable characteristics such as featureless angular distributions and complicated distorted-wave analyses, frequently exacerbated by multi-step processes.

Because until recently few accelerators have been capable of providing suitable beams, there has been relatively little experimental work involving two-proton pickup and, as yet, no single reaction has emerged as being especially suitable. Reactions which have been used for which only limited experience is available include (^{6}Li, ^{8}B) [refs. [3,4])], (^{11}B, ^{13}N) [ref. [5])], (^{14}C, ^{16}O) [ref. [6])], and (^{18}O, ^{20}Ne) [ref. [7])]. The latter reaction has the disadvantage that excitation of low-lying states in ^{20}Ne often results in spectra complicated by overlapping "shadow" peaks. Based on recent studies [6]) using targets of Ti and Cr, the (^{14}C, ^{16}O) reaction appears to be one of the most promising for experiments requiring pickup of two protons. The angular distributions exhibit a characteristic L-dependence and, since the first excited states in both ^{14}C and ^{16}O occur above 6 MeV excitation, spectra contamination from projectile and ejectile excitation should be minimized.

There have been but a few reports [3,4]) in the literature concerning the (^{6}Li, ^{8}B) reaction, which is the lightest of the many possible two-proton pickup reactions, and only one investigation [4]) of its spectroscopic utility, this on four 1p shell targets. This reaction, therefore, warrants further study as to its suitability for experiments requiring two-proton pickup. An attractive feature of the (^{6}Li, ^{8}B) reaction is that ^{8}B ions are easily identified since both of the two neighboring isotopes, ^{7}B and ^{9}B, are proton unbound. And, unlike some other reactions such as (^{18}O, ^{20}Ne), there are no shadow-peak ambiguities as ^{8}B has no particle-stable excited states.

This paper has as its focus two main points. We present first our results from a spectroscopic study in the Zr region using the (^{6}Li, ^{8}B) two-proton pickup reaction and then, our conclusions concerning the applicability of this reaction as a spectroscopic tool. Several reasons make Zr and environs attractive for investigation. For the states of interest in this paper, mainly the low-lying 0^+ and 2^+ states, the structure is relatively simple and understood theoretically. The amplitudes in the Zr g.s. wave functions have been determined by single-proton stripping and pickup experiments [8,9]) and can be compared directly with the amplitudes determined by the (^{6}Li, ^{8}B) reaction. Transitions in the Zr region, where protons are filling the $f_{\frac{5}{2}}$, $p_{\frac{3}{2}}$, $p_{\frac{1}{2}}$, and $g_{\frac{9}{2}}$ orbitals, are enhanced by the "hot-orbit" effect, wherein the cross-section for pickup of a pair from an orbital of low l is often substantially larger than that from orbitals of high l. For example, calculations for the Mo(^{6}Li, ^{8}B)Zr reaction indicate that the cross section for $(p_{\frac{1}{2}})^2$ pickup is approximately five times larger when compared to pick-

up of a pair from the $g_{\frac{9}{2}}$ orbital. An additional reason for investigating this region is the availability of α-pickup data obtained from a recent (d, ^{6}Li) experiment [10]) on four targets of Mo. It has been shown by Kurath and Towner [11]) that many properties of α-transfer reactions can be related to the behavior of two-nucleon transfer reactions. Therefore, it is of considerable interest to look for correlations between the (d, ^{6}Li) results, existing (p, t) data, and the (^{6}Li, ^{8}B) results obtained in the present work.

The experimental procedures and results are presented in sects. 2 and 3. Details of the DWBA analysis are given in sect. 4, followed by a discussion of the results and conclusions in sect. 5. An earlier account of a portion of this work concerning transitions to levels in ^{92}Zr and ^{96}Zr has been published elsewhere [12]).

2. Experimental description

The experiments were performed at the Indiana University cyclotron facility (IUCF) and used energy-analyzed beams of 90 MeV ^{6}Li ions to bombard isotopically-enriched, self-supporting targets of molybdenum and zirconium. The properties of these targets are listed in table 1. Time-averaged beam currents were typically 40–50 enA.

TABLE 1

Properties of targets

Target	Isotopic composition		Thickness (mg/cm^2)	Approximate resolution (keV) [a])	Target	Isotopic composition		Thickness (mg/cm^2)	Approximate resolution (keV) [a])
	mass	%				mass	%		
^{92}Mo	92	98.3	0.590	262	^{100}Mo	96	0.8	0.818	362
	94	0.5				98	1.7		
						100	95.9		
^{94}Mo	92	0.9	1.03	456	^{90}Zr	90	97.6	0.585	264
	94	93.9				91	1.0		
	95	2.9				92	0.7		
	96	1.0				94	0.6		
^{96}Mo	95	0.9	0.593	263	^{92}Zr	90	2.5	0.506	228
	96	96.8				91	1.0		
	97	1.0				92	95.1		
						94	1.1		
^{98}Mo	96	0.6	0.418	184	^{94}Zr	90	0.9	0.537	242
	97	0.8				92	0.8		
	98	97.0				94	97.6		
	100	0.6							

[a]) In these experiments, the energy resolution is determined mainly by energy losses in the target. A rough approximation of the resolution is taken to be the difference in target dE/dx for ^{8}B and ^{6}Li times the target thickness.

The ^{8}B ejectiles were momentum analyzed in a QDDM magnetic spectrograph and detected in a position-sensing gridded ionization chamber placed at the focal plane of the spectrograph.

The ion chamber is similar in concept to those constructed at Argonne [13]) and Rochester [14]), though larger in size. With a useful length of 45 cm and a depth of $\sim$ 25 cm, the detector covers the entire focal surface of the IUCF spectrograph and, when filled with one atmosphere of isobutane, can stop 295 MeV ^{16}O ions incident at 45°. An important advantage of chambers of this type is the "clean" design; after passing through the entrance window (12.7 μm mylar when using 0.6 atm of isobutane), there are no grids or foils which the ion must traverse with the resulting degradation of the energy resolution. When an ion enters the chamber, there is an initial measurement of position by a position-sensitive proportional counter (PSPC) located on the focal plane followed by two sequential measurements of the differential energy loss dE/dx, a second position measurement which can be used to determine the angle of incidence, and a simultaneous measurement of the total energy deposited in the active region. A third proportional counter mounted at the rear of the chamber serves as a veto counter for passing particles. The two PSPC, from which position is determined using the Borkowski-Kopp rise time scheme [15]), are separated by a distance of 10 cm along the ion path. For each event, the energy, the two differential energy-loss signals, and the two position signals from the ionization chamber could be recorded on magnetic tape in event mode and simultaneously sorted on-line. Usually one position signal and one ΔE signal were sufficient. In two-dimensional displays of E versus ΔE, the ^{8}B events were clearly separated from those of other ion species.

Spectra were recorded at 8° for all targets with a ^{6}Li beam energy of 90 MeV. In addition, angular distributions for the transitions to the g.s. and 2_1^+ level of ^{88}Sr were measured out to 30°. The horizontal acceptance angle of the spectrograph was set at $\pm$ 1.3° providing a solid angle of 3.3 msr. The major contributor to the energy resolution was the ^{8}B energy loss in the targets, typically $\sim$ 600 keV/mg·cm^{-2}. When expressed in keV, the difference in target energy loss for ^{8}B and ^{6}Li gives a rough approximation of the energy resolution and is listed for each target in table 1.

3. Experimental results

3.1. THE Mo(^{6}Li, ^{8}B)Zr REACTIONS

The ^{8}B energy spectra obtained at $\theta_{lab} = 8°$ for five even-A Mo targets are shown in fig. 1. The spectra cover at least 3 MeV of excitation. The ^{100,98}Mo(^{6}Li, ^{8}B)^{98,96}Zr reactions have the most negative Q-values, -13.7 and -11.5 MeV respectively. Thus there are no impurity peaks in any of the five spectra arising from reactions on ^{12}C and ^{16}O contaminants, which have Q-values of -21.4 and -16.6 MeV respectively. Although, with one exception, angular distributions were not measured for the Mo or Zr targets, it is believed they would be similar to those we have observed, for com-

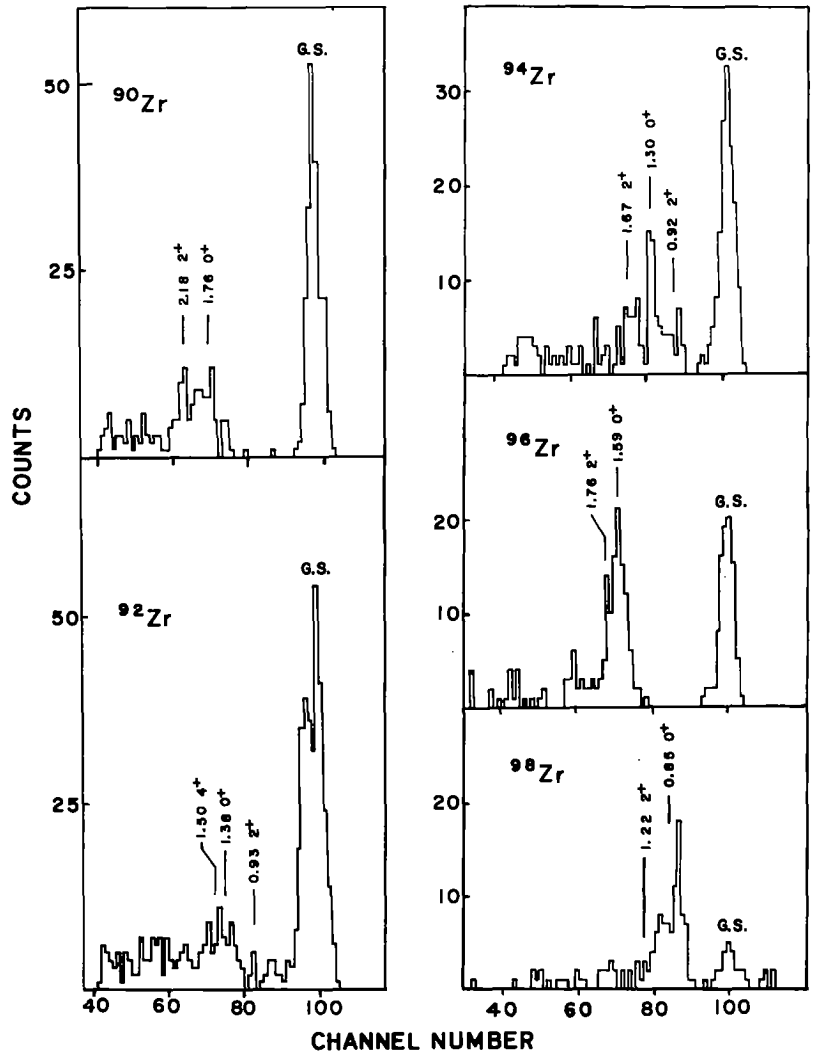

Fig. 1. Spectra at 8° lab from the ^{92,94,96,98,100}Mo(^{6}Li, ^{8}B)^{90,92,94,96,98}Zr reactions at 90 MeV. Note the relative strength of the 0_2^+ to the g.s. in ^{98}Zr as compared to ^{90}Zr.

parable Q-values and bombarding energy, in the ^{90}Zr(^{6}Li, ^{8}B)^{88}Sr reaction. In that case the angular distributions for the g.s. and 2_1^+ state, as shown in fig. 3, are featureless and fall off rapidly with increasing angle. In the ^{90,92,94}Zr spectra the $0^+ \rightarrow 0^+$ transition to the g.s. is the dominant peak while the 0_2^+ is relatively less intense. In ^{96,98}Zr, on the other hand, the 0_2^+ transition is more pronounced and is, in fact, the dominant peak in the ^{98}Zr spectrum. As will be shown below, the variation in 0_2^+ strength relative to that of the g.s. can be traced to systematic changes with

TABLE 2

Transitions to 0^+ states in Zr

Target nucleus	Final nucleus	Excitation [a]) (MeV)	$\sigma_{c.m.}(8.6°)$ (μb/sr)	α, β [b])	$\sigma(0_2^+)/\sigma_{g.s.}$ [c])	$\sigma(0_2^+)/\sigma_{g.s.}$ [d])
^{100}Mo	^{98}Zr	0.0	1.6 ± 0.2	0.98, 0.20	2.1	2.1
		0.853	3.4 ± 0.5			
^{98}Mo	^{96}Zr	0.0	5.6 ± 0.9	0.95, 0.32	0.96	1.22
		1.594	5.4 ± 1.2			
^{96}Mo	^{94}Zr	0.0	9.6 ± 1.3	0.81, 0.59	0.24	0.35
		1.300	2.3 ± 0.5			
^{94}Mo	^{92}Zr	0.0	19.9 ± 2.6	0.71, 0.71	0.21	0.17
		1.383	4.1 ± 1.1			
^{92}Mo	^{90}Zr	0.0	24.7 ± 3.3	0.77, 0.64	0.26	0.32
		1.761	6.3 ± 1.4			

[a]) Excitation energies quoted in this work were taken from published sources.
[b]) Amplitudes in the Zr g.s. wave function used in DWBA calculations. See sect. 5 for details.
[c]) Experimentally determined ratio of transition strengths.
[d]) Calculated ratio of transition strengths.

neutron number of the Zr proton configurations. In general, $0^+ \rightarrow 0^+$ transitions dominate the spectra while other states, e.g. low-lying 2^+ and 3^- levels, are only weakly populated. In table 2 the measured c.m. differential cross sections at $\theta_{c.m.} = 8.6°$ are listed for states in the five final Zr nuclei. Other entries in the table will be discussed later.

The uncertainties in the absolute cross sections quoted in tables 2 and 3 are attributable mainly to counting statistics, uncertainties in target thickness, and for some of the excited-state transitions, uncertainties in peak separation where levels were

TABLE 3

Transitions to states in Sr

Target nucleus	Final nucleus	Excitation [a]) (MeV)	I^π	$\sigma_{c.m.}(8.6°)$ (μb/sr)
^{94}Zr	^{92}Sr	0.0	0^+	7.3 ± 1.1
		0.815	2^+	2.3 ± 0.5
^{92}Zr	^{90}Sr	0.0	0^+	15.1 ± 2.2
		0.832	2^+	1.8 ± 0.5
^{90}Zr	^{88}Sr	0.0	0^+	22.1 ± 3.0
		1.836	2^+	14.1 ± 1.8

[a]) Excitation energies quoted in this work were taken from published sources.

not fully resolved. Typically the exposures were chosen to put several hundred events in the g.s. peaks.

Because of the connection between α-pickup and two-neutron and two-proton pickup, it is of interest to point out the similarities and differences in the spectra observed in the (d, ^{6}Li), (p, t), and (^{6}Li, ^{8}B) reactions. Insofar as transitions to the g.s. and 0_2^+ states are concerned, spectra [10]) from the ^{94,96,98,100}Mo(d, ^{6}Li)^{90,92,94,96}Zr reactions at 45 MeV are qualitatively similar to those observed in the present work. In particular, relative to the g.s. the 0_2^+ in the ^{96}Zr is strongly excited while it is weak in the lighter-mass isotopes. Compared to (^{6}Li, ^{8}B), the (d, ^{6}Li) spectra are somewhat richer – populating more states with greater intensity – and, for some of the 2^+ and 3^- states, the intensities are comparable to that of the 0_2^+. This is not unexpected as the (d, ^{6}Li) reaction can populate states not only through their proton components but through their neutron components as well.

We can also compare the present results with spectra from the ^{92,94,96}Zr(p, t)^{90,92,94}Zr reactions [16]) at 38 MeV. The (p,t) two-neutron pickup reaction is

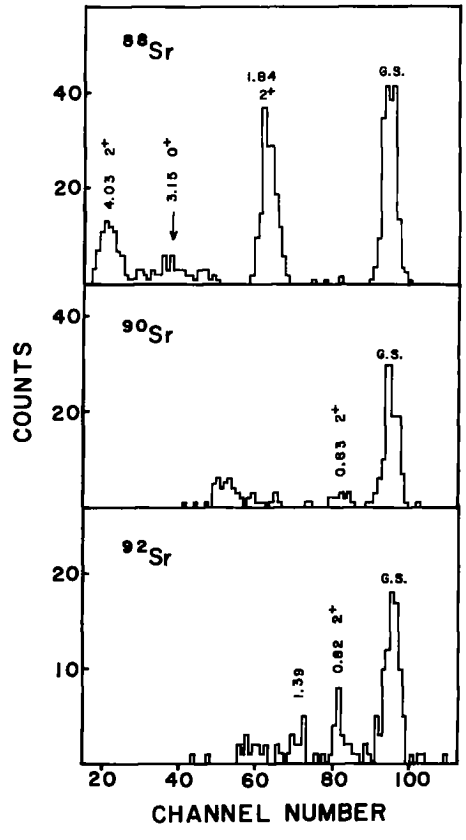

Fig. 2. Spectra at 8° lab from the ^{90,92,94}Zr(^{6}Li, ^{8}B)^{88,90,92}Sr reactions at 90 MeV.

particularly sensitive to the neutron structure of the Zr wave functions but relatively insensitive to the proton structure. The spectra are dominated by strong g.s. transitions which are usually 5 to 10 times stronger than any of the other transitions. The 0_2^+ states in ^{90,92,94}Zr are among the weakest states populated, whereas transitions to these same states are more intense in both (d, ^{6}Li) and (^{6}Li, ^{8}B). This seems to reinforce the conclusion [16,17]) that the lowest excited 0^+ state in the Zr isotopes is mainly a proton excitation.

3.2. THE Zr(^{6}Li, ^{8}B)Sr REACTIONS

The ^{8}B energy spectra obtained at $\theta_{lab} = 8°$ for three even-A Zr targets are shown in fig. 2. As with the Mo targets, there are no contaminant peaks from ^{12}C or ^{16}O in the first 3 MeV of excitation because of Q-value differences. The c.m. differential cross sections are given in table 3. A striking new feature is present in the ^{88}Sr spectrum – a very strong transition to the 2_1^+ state. In fact, in the Sr isotopes, the 2_1^+ states are more strongly populated than the 0_2^+ states, which is the reverse of the situation in the Zr isotopes. Due to the absence of stable targets, it is not possible to compare two-neutron pickup from the (p, t) reaction with the (^{6}Li, ^{8}B) results. A comparison can be made, however, with the ^{92}Zr(d, ^{6}Li)^{88}Sr reaction [18]) at 33 MeV which also shows a strong transition to the 2_1^+ state at 1.84 MeV. At $\theta_{lab} = 14°$, the 2_1^+ state is the strongest peak in the spectrum, approximately twice as intense as the g.s. transition.

The only angular distributions taken in this work were of transitions to the g.s. and

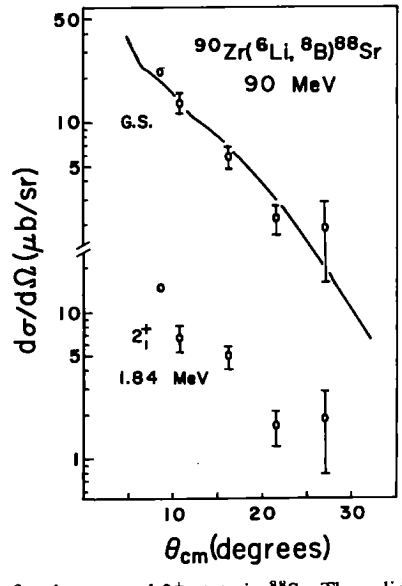

Fig. 3. Angular distributions for the g.s. and 2_1^+ state in ^{88}Sr. The solid curve is a normalized DWBA prediction.

2_1^+ in ^{88}Sr. As can be seen in fig. 3, the angular distributions are essentially structureless and drop off rapidly with increasing angle. In judging the usefulness of the (^{6}Li, ^{8}B) reaction, it is important to note that there is no significant difference in the shapes of these two angular distributions, which makes it impossible, on this basis, to distinguish between $0^+ \rightarrow 0^+$ and $0^+ \rightarrow 2^+$ transitions.

4. DWBA analysis

To obtain a theoretical prediction for the measured strengths of the $0^+ \rightarrow 0^+$ transitions, we have performed exact finite-range distorted-wave Born approximation (EFR DWBA) calculations using the computer code DWUCK5 [ref. [19]]. We have assumed that the (^{6}Li, ^{8}B) reaction can be adequately described as a direct, one-step transfer of a cluster of two protons in a $T = 1, S = 0$ state. The details of the formalism are outlined in the appendix.

The ^{6}Li and ^{8}B optical-model parameters are listed in table 4. The entrance channel parameters were obtained from an analysis of 99 MeV ^{6}Li ions elastically scattered from ^{90}Zr [ref. [20]]. Because ^{8}B is unstable, data from ^{8}B elastic scattering are not available; hence parameters from the elastic scattering of ^{11}B from ^{208}Pb at 72 MeV [ref. [21]] were substituted.

The bound-state wave functions describing the motion of the two-proton cluster in ^{8}B and the target nuclei were generated with a Woods-Saxon shape nuclear potential and a Coulomb potential. The number of radial nodes and the orbital angular momentum of the cluster were determined from a microscopic analysis using shell-model wave functions for the projectile-ejectile and target-residual pairs. The depth of the Woods-Saxon potential was varied so as to bind the transferred cluster at the measured two-proton separation energy.

The dependence of the cross section on the nuclear wave functions is contained in the spectroscopic amplitudes, A_{cB} and A_{cb} in eq. (A.4). The amplitude for the projectile-ejectile pair, A_{cb}, was calculated from two-proton coefficients of fractional parentage (c.f.p.) for ^{8}B(2^+) $\rightarrow$ ^{6}Li(1^+) + 2p, appropriate for the (^{6}Li, ^{8}B) reaction. In light-ion two-nucleon transfer reactions such as (p, t) or (^{3}He, n), the nucleons are transferred predominantly in relative ^{1}S states, from which it follows that the wave function for the transferred pair must be spatially symmetric. In reactions with heavy ions, however, it has been pointed out by both Rotter [22]) and Kurath [23]) that spatially antisymmetric transfer may also be significant. Thus in the (^{6}Li, ^{8}B) reaction, the dominant c.f.p.'s allow the two protons captured by the ^{6}Li projectile to be in either a symmetric (^{1}D) or antisymmetric (^{3}P) state relative to the ^{6}Li core. In fact for this reaction, antisymmetric transfer could conceivably play a major role, since according to the calculation of Elliot *et al.* [24]) the ^{3}P amplitude exceeds that of the ^{1}D component by more than 30 percent.

The importance of spatially antisymmetric transfer was investigated by Weisenmiller *et al.* [4]) in a study of the (^{6}Li, ^{8}B) reaction on four 1p shell targets. They observed that transitions are very weak to levels that can be populated only via

antisymmetric transfer and hence conclude that this transfer mode is probably not important. Following this result, in our calculations we have considered only spatially symmetric (and hence spin-singlet) states for the transferred proton pair. This assumption, that only the ^{1}D component of the two-proton ^{8}B c.f.p. contributes significantly to the reaction, simplifies the analysis by requiring the two transferred protons to have antiparallel spins ($S = 0$) and restricting their relative motion to 0s and 0d orbital angular momentum states. Although both these possibilities for the relative motion were included in preliminary calculations, it was found that the 0s contribution to the cross section uniformly exceeded that of the 0d by more than an order of magnitude. Thus in the calculations compared with the data, only the 0s amplitude was included. This further simplification results in a calculation similar to the usual one for (p, t) and (t, p), except that finite-range effects, and the $L = 2$ motion of the proton cluster relative to the ^{6}Li core, are taken into account. As will be pointed out in sect. 5, there is a good agreement between the DWBA predictions and the measured values of relative cross sections, which tends to support the validity of this simple model.

The spectroscopic amplitudes for the Mo-Zr pairs were calculated assuming a pure $(p_{\frac{1}{2}})^2(g_{\frac{9}{2}})^2$ proton configuration for the Mo ground states. As in the analysis of Mo(d, ^{6}Li) cross sections by Saha *et al.* [10]), we have assumed the proton configuration of the Zr ground states to be of the form $\alpha(p_{\frac{1}{2}})^2 + \beta(g_{\frac{9}{2}})^2$. The first excited 0^+ states in Zr are taken to be the orthogonal states $\beta(p_{\frac{1}{2}})^2 - \alpha(g_{\frac{9}{2}})^2$. Calculations of the amplitudes for the Zr-Sr pairs assumed an inert proton configuration with filled $1f_{\frac{7}{2}}$ and $2p_{\frac{3}{2}}$ orbitals for the Sr ground states. In a study [9]) of the (^{3}He, d) single-proton stripping reaction on all the stable Zr isotopes, it was concluded that for the Zr ground states, the $2p_{\frac{3}{2}}$ proton orbital appears to be about 90 % filled while the $1f_{\frac{5}{2}}$ is about 96 % filled. It therefore seems reasonable to regard Sr as an inert proton core and, in fact, shell-model calculations based on this assumption are able to account for many features of the Zr isotopes.

^{90}Zr has an $N = 50$ neutron configuration which is filled through the $1g_{\frac{9}{2}}$ orbital and is known to form a good major closed shell. The first neutron orbital lying above the $N = 50$ closed shell is the $2d_{\frac{5}{2}}$. A substantial gap is expected between this orbital and the next, the $3s_{\frac{1}{2}}$. Up to $N = 56$, where the $d_{\frac{5}{2}}$ orbital is filled, (t, p) data [25]) suggest that the neutron configurations of the low-lying levels are relatively simple, being predominantly $(2d_{\frac{5}{2}})$. In all of our calculations, we have assumed the neutrons to be inert.

For the (p, t) and (t, p) reactions, one finds that EFR DWBA calculations [26]) are able to predict the shapes of angular distributions rather well although absolute magnitudes of the cross sections are consistently underestimated. We have observed similar results in our analysis of the (^{6}Li, ^{8}B) reaction. While our calculations are able to reproduce relative cross sections, the absolute magnitudes are under-predicted, typically by an order of magnitude. Although we have refrained from doing so, it is likely some improvement could be obtained by arbitrary adjustments in the DWBA parameters.

5. Results and discussion

The EFR DWBA code DWUCK5 was used to calculate the ratio of the cross section for the first excited 0^+ state to that of the ground state in all five Zr nuclei. The calculated cross section ratios depend sensitively on the choice of spectroscopic amplitudes for the (Mo, Zr) pair, but should be relatively less sensitive to uncertainties in the potential parameters used in the analysis. A comparison of the calculated and experimental ratios is given in table 2, and graphically in the upper part of fig. 4, where it can be seen that the agreement is quite good.

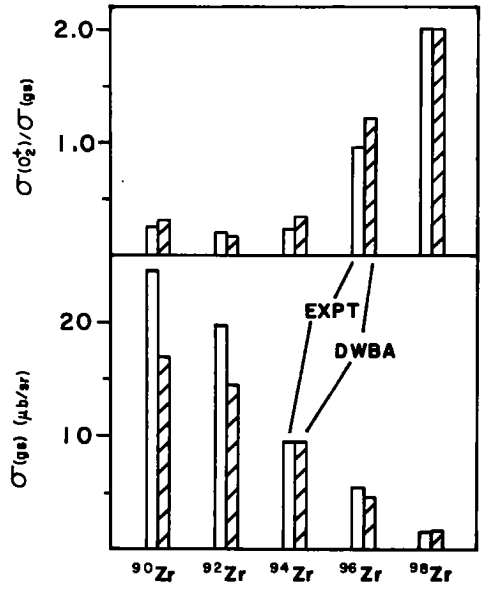

Fig. 4. In the upper part, a comparison is made between DWBA prediction and experiment for the ratio of (^{6}Li, ^{8}B) transition strengths to the 0_2^+ and g.s. in Zr. The details of the DWBA calculations are described in the text. In the lower part there is a comparison of measured and calculated c.m. differential cross sections at $\theta_{lab} = 8°$, normalized to one another at mass number 94.

The amplitudes α and β in the assumed Zr g.s. proton configurations $[\alpha(p_{\frac{1}{2}})^2 + \beta(g_{\frac{9}{2}})^2]$ which were used in the calculations are also listed in table 2. Except for ^{98}Zr, these amplitudes have been determined from single-proton pickup [8]) and stripping data [9]) and are based on averages of the experimentally obtained values given in table 13 of ref. [9]). Due to the absence of stable targets, the single-proton pickup and stripping data necessary to extract the wave function coefficients α and β for ^{98}Zr are unavailable. Therefore they were adjusted in the calculations to yield a cross section ratio equal to that observed experimentally in this work and, as such, represent the first experimental determination of these amplitudes. To illustrate the precision with which the wave function amplitudes for ^{98}Zr can be extracted from the (^{6}Li, ^{8}B) data, in the

DWBA calculations a 1 % change in α results in a 15 % change in the 0_2^+/g.s. cross-section ratio.

The principal feature of the five Zr spectra, which is clearly reflected in fig. 4, is the large increase in 0_2^+ strength relative to that of the g.s. which is observed going toward the heavier isotopes. In ^{90}Zr, the 0_2^+ transition is weak whereas it is the dominant transition in ^{98}Zr, with twice the g.s. strength. A variation of this magnitude in the 0_2^+/g.s. cross-section ratio, which suggests a change in the proton configuration, might at first seem surprising since it is the number of neutrons, not protons, that is changing. Saha *et al.* [10]) first observed this variation in the α-pickup reactions Mo(d, ^{6}Li) Zr and argued qualitatively that changes in the Zr proton configurations were the underlying cause. This is confirmed by our (^{6}Li, ^{8}B) results, which are understandable in terms of DWBA calculations and which are not as directly influenced by changes in the Zr neutron configurations. The rather dramatic increase in 0_2^+ strength observed in ^{96,98}Zr is attributable to the larger g.s. occupancy of the "hot" $2p_{\frac{1}{2}}$ orbital in these heavier Zr isotopes. For the g.s. transition, this implies an increased probability for pickup of proton pairs from the "cold" $1g_{\frac{9}{2}}$ orbital in the Mo target and a corresponding decrease in the $2p_{\frac{1}{2}}$ amplitude, resulting in reduced transition strength. Since in our model the wave function for the 0_2^+ state is orthogonal to that of the g.s., the reverse situation prevails for this state and its transition strength is increased. Qualitative numerical estimates which also agree well with experiment were compared in ref. [12]) for the 0_2^+/g.s. cross-section ratios in ^{92,96}Zr.

In the lower half of fig. 4 we compare measured and calculated c.m. differential cross sections for the g.s. transitions, normalized to one another at mass number 94. The A-dependence is not fully reproduced by the DWBA results; for $A = 90$, the normalized calculation is less than experiment by 30 %.

The (Zr/Sr) spectra are distinctly different from those obtained with the Mo targets in that the prominent transitions to excited 0^+ states have been replaced by $0^+ \rightarrow 2^+$ transitions. The transition strength to the excited 2^+ level at 1.84 MeV in ^{88}Sr is comparable to that of the g.s. transition, in contrast to the much weaker 2^+ transitions in ^{90,92}Sr. This may be attributable in part to the $N = 50$ closed shell neutron configuration in ^{88}Sr which could reduce the mixing of the 2^+ proton strength with 2^+ neutron states. In fig. 3, the solid curve is the DWBA prediction normalized to the angular distribution for the ^{90}Zr(^{6}Li, ^{8}B)^{88}Sr g.s. transition. It can be seen that the featureless character and overall slope of the measured angular distribution are well reproduced by the calculation.

In a study [27]) of the ^{86}Kr(^{3}He, n)^{88}Sr reaction, a strong transition was observed leading to the 0^+ state at 3.15 MeV in ^{88}Sr with about one-third of the strength expected for the transition to the pairing vibration if the proton subshell is closed at $Z = 38$. Later calculations [28]) have confirmed the identification of this level as the proton pairing vibration at the $Z = 38$ subshell closure. It is interesting to note that this level is not strongly excited in the ^{90}Zr(^{6}Li, ^{8}B)^{88}Sr reaction.

One purpose of this investigation has been to evaluate the suitability of the (^{6}Li, ^{8}B)

reaction for studies of two-proton pickup. We conclude with some remarks regarding this question.

The (^{6}Li, ^{8}B) reaction is attractive experimentally because of the ease with which ^{8}B ions can be identified and because, in comparison with reactions involving heavier ions, kinematic and Coulomb barrier effects are less pronounced and energy loss in the target is minimized.

The reaction appears to be highly selective, with 0^+ states normally favored. In addition to the measurements discussed in this paper, we have previously measured (^{6}Li, ^{8}B) spectra at 90 MeV and $\theta_{lab} = 8°$ from ^{56}Fe, ^{66}Zn, and ^{120,126,130}Te targets [29]). In these examples the laboratory cross section for the g.s. transition ranged from 27 μb/sr for the ^{66}Zn target to 0.3 μb/sr for ^{130}Te. Thus the yield, although smaller than is observed for light-ion two-nucleon transfer reactions such as (p, t), is comparable to that for (d, ^{6}Li), which has been extensively used in studies of nuclear structure.

Perhaps the greatest disadvantage of the (^{6}Li, ^{8}B) reaction as a probe of nuclear structure is that (at 90 MeV) the angular distributions are featureless and cannot be used to infer the L-transfer, even for $0^+ \rightarrow 0^+$ transitions. However, in the present case at least, the close agreement between the calculated and experimental cross-section ratios for these transitions suggests that the reaction is adequately described by assuming the direct transfer of a $T = 1$, $S = 0$ proton pair. As mentioned in sect. 4, previous work with lighter, 1p shell targets [4]) has led to the same conclusion. As a consequence of this assumption the relative motion of the proton pair is restricted to symmetric 0s and 0d orbital angular momentum states. Moreover the dominant contribution of the former to the predicted cross sections leads to a calculation similar to that for (t, p) and (^{3}He, n), in which the two nucleons are transferred in a 0s relative state.

Comparing the (^{6}Li, ^{8}B) reaction with the other possible two-proton pickup reactions which have been investigated, the (^{14}C, ^{16}O) reaction appears to be a particularly promising alternative. At 51 MeV on targets in the $A = 50$ region [6]), the latter reaction has been found to yield angular distributions which are indicative of the L-transfer, with cross sections that are substantially larger than we have found [29]) for the (^{6}Li, ^{8}B) reaction on comparable targets. These features are probably due in part to the positive Q-values for the (^{14}C, ^{16}O) reaction, which are kinematically more favorable than the (^{6}Li, ^{8}B) Q-values. Apart from the difficulty of producing a ^{14}C beam [30]) and the higher bombarding energies which would be required in the study of heavier nuclei, (^{14}C, ^{16}O) is therefore likely to be the more versatile of the two reactions. However, the experimental convenience of the (^{6}Li, ^{8}B) reaction, and the success of the straightforward cluster-model treatment in describing the present experiments, suggests that this reaction would be a useful spectroscopic tool in cases where $0^+ \rightarrow 0^+$ transitions are of primary interest.

We thank F. D. Becchetti and J. Jänecke for making available to us their version of the finite-range code DWUCK5. Also we thank K. T. Hecht for several helpful

discussions. Two of us (R.S.T. and W.S.G.) were supported by grants from the Michigan Memorial Phoenix Project and the Rackham Graduate School of The University of Michigan.

Appendix

FORMALISM USED FOR THE (^{6}Li, ^{8}B) REACTION

In this appendix we outline the theory used in calculating cross sections for two-proton pickup with the (^{6}Li, ^{8}B) reaction. The formalism is based on the calculations of α-transfer reactions by Kurath and Towner [11]) and, in particular, its adaptation by Becchetti [31]) to ^{8}Be pickup.

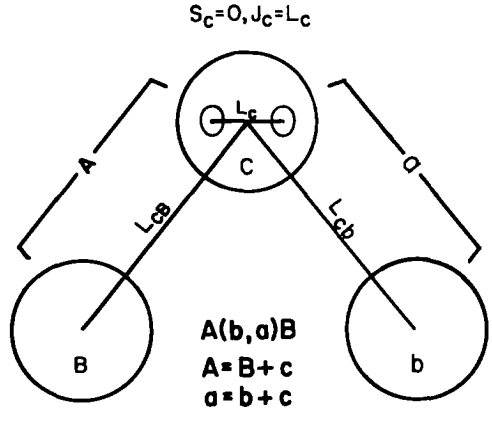

Fig. 5. Schematic representation of the coupling between the two-proton cluster and the core: A = target nucleus, B = residual nucleus, a = ^{8}B, b = ^{6}Li, c = two-proton cluster.

Fig. 5 shows schematically the cluster core couplings for the pickup of a two-proton cluster in the A(b, a)B reaction. For reasons discussed in the text, we consider only cases in which the two protons (≡ c) are in an $S_c = 0$ spin-singlet state. As a consequence, the two protons picked up by the ^{6}Li projectile are restricted by the two-proton c.f.p. for ^{8}B to be in a ^{1}D state relative to the ^{6}Li core. In this state, the two p-shell protons can be, with equal probability, in 0s or 0d angular momentum states relative to each other. We represent their relative angular momentum by $\boldsymbol{J}_c = \boldsymbol{L}_c + \boldsymbol{S}_c = \boldsymbol{L}_c$ where $L_c = 0$ or 2. The orbital angular momentum of the cluster relative to the residual nucleus B (the inert core of the target) is denoted as L_{cB}; relative to ^{6}Li (≡, b), it is L_{cb}. For an even-even target ($J^\pi_A \equiv 0^+$), we can write $\boldsymbol{J}_B = \boldsymbol{L}_c + \boldsymbol{L}_{cB}$ and $\boldsymbol{J}_a = \boldsymbol{L}_c + \boldsymbol{L}_{cb} + \boldsymbol{J}_b$ where $J^\pi_a(^8\mathrm{B}) = 2^+$ and $J^\pi_b(^6\mathrm{Li}) = 1^+$. The number of radial nodes, N, used to characterize the motion of the cluster c relative to the cores B and b, is taken from the relations [11]) $2N_{cB} + L_{cB} = Q_{cB}$ and $2N_{cb} + L_{cb} = Q_{cb}$, where Q_{cB} and Q_{cb} are the number of oscillator quanta implied by the shell-model configuration of the two protons in the target or in ^{8}B respectively.

The cross section for direct pickup of a two-proton cluster is given by

$$\frac{d\sigma}{d\Omega} = \frac{\mu_{aB}\mu_{bA}}{(2\pi\hbar^2)^2}\,\frac{k_{aB}}{k_{bA}}\,\frac{1}{2s_b+1}\sum_{LM}\Big|\sum_{\substack{L_{cB}L_{cb}\\ N_{cB}N_{cb}}} B_{cB}\beta_{LM}\Big|^2, \tag{A.1}$$

where

$$\beta_{LM} = \frac{(-1)^L}{\sqrt{2L+1}}\int d\boldsymbol{r}_{bA}d\boldsymbol{r}_{aB}\chi^*(\boldsymbol{r}_{bA})\chi(\boldsymbol{r}_{aB})f_{LM}(\boldsymbol{r}_{cb},\boldsymbol{r}_{cB}), \tag{A.2}$$

$$f_{LM} = \sum_{\Lambda\bar{\Lambda}}(-1)^{L_{cb}+\bar{\Lambda}}\{L_{cB}\Lambda L_{cb}-\bar{\Lambda}|LM\rangle\Phi^*_{\Lambda}(\boldsymbol{r}_{cB})V(\boldsymbol{r}_{cb})\Phi_{\bar{\Lambda}}(\boldsymbol{r}_{cb}), \tag{A.3}$$

$$B_{cB} = i^L\sum_{L_c}\left(\frac{2J_a+1}{2L_c+1}\right)^{\frac{1}{2}}(-1)^{L_{cB}+L_c-J_B}U(J_BL_{cB}J_aL_{cb};L_cL)A^*_{cB}A_{cb}. \tag{A.4}$$

The dependence on kinematics and the reaction mechanism is contained in the factor β_{LM}, where $f_{LM}(\boldsymbol{r}_{cb},\boldsymbol{r}_{cB})$ is the finite-range form factor. The spectroscopic dependence lies in the factor B_{cB} and the two spectroscopic amplitudes A_{cB} and A_{cb} contained therein. In the calculations we have assumed that during the transfer the relative motion of the two protons is unchanged, i.e. L_c = constant. Therefore, as mentioned above, the structure of ^{8}B restricts the sum over L_c in the factor B_{cB} to just two values, $L_c = 0,\ 2$. For $0^+ \to 0^+$ transitions, the orbital angular momentum transfer $\boldsymbol{L} = \boldsymbol{L}_{cB} - \boldsymbol{L}_{cb}$ thus has but one value, $L = 2$. As we have mentioned in sect. 4, the $L_c = 0$ contribution to the amplitude β_{LM} was found to dominate that of $L_c = 2$. Consequently only the former was used in the calculations which were compared with the data.

References

1) M. A. Oothoudt and N. M. Hintz, Nucl. Phys. **A213** (1973) 221;
H. W. Baer, J. J. Kraushaar, C. E. Moss, N. King, R. Green, P.D. Kunz and E. Rost, Ann. of Phys. **76** (1973) 437;
E. R. Flynn, R. A. Broglia, R. Liotta and B. S. Nilsson, Nucl. Phys. **A221** (1974) 509;
C. Ellegaard, J. D. Garrett and J. R. Lien, Nucl. Phys. **A307** (1978) 125;
H. Kusakari, K. Kitao, S. Kono and Y. Ishizaki, Nucl. Phys. **A341** (1980) 206;
E. R. Flynn and D. G. Burke, Phys. Rev. **C17** (1978) 501;
R. A. Broglia, O. Hansen and C. Riedel, in Advances in nuclear physics, vol. 6 (Plenum, New York, 1973) p. 357, and references therein

2) F. D. Becchetti, D. G. Kovar, B. G. Harvey, D. L. Hendrie, H. Homeyer, J. Mahoney, W. von Oertzen and N. K. Glendenning, Phys. Rev. **C9** (1974) 1543;
D. G. Kovar, W. Henning, B. Zeidman, Y. Eisen, J. R. Erskine, H. T. Fortune, T. R. Ophel, P. Sperr and S. E. Vigdor, Phys. Rev. **C17** (1978) 83;
P. P. Tung, K. A. Erb, M. W. Sachs, G. B. Sherwood, R. J. Ascuitto, and D. A. Bromley, Phys. Rev. **C18** (1978) 1663

3) N. A. Jelley, K. H. Wilcox, R. B. Weisenmiller, G. J. Wosniak and J. Cerny, Phys. Rev. **C9** (1974) 2067; R. B. Weisenmiller, N. A. Jelley, D. Ashery, K. H. Wilcox, G. J. Wosniak, M. S. Zisman and J. Cerny, Nucl. Phys. **A280** (1977) 217
4) R. B. Weisenmiller, N. A. Jelley, K. H. Wilcox, G. J. Wosniak and J. Cerny, Phys. Rev. **C13** (1976) 1330
5) B. G. Harvey, D. L. Hendrie, L. Kraus, C. F. Maguire, J. A. Mahoney, D. K. Scott, Y. Terrien and K. Yagi, Int. Conf. on reactions between complex nuclei, Nashville, 1974, ed. R. L. Robinson, F. K. McGowan, J. B. Ball and J. H. Hamilton (North-Holland, Amsterdam, 1974) p. 142;
D. K. Scott, B. G. Harvey, D. L. Hendrie, L. Kraus, C. F. Maguire, J. Mahoney, Y. Terrien and K. Yagi, Phys. Rev. Lett. **33** (1974) 1343
6) J. C. Peng, N. Stein, J. W. Sunier, D. M. Drake, J. D. Moses, J. A. Cizewski and J. R. Tesmer, Phys. Rev. Lett. **43** (1979) 675
7) H.-P. Rother, W. Henning, H.-J. Körner, R. Müller, K. E. Rehm, M. Richter and H. Spieler, Nucl. Phys. **A269** (1976) 511;
R. H. Siemssen, C. L. Fink, L. R. Greenwood and H. J. Körner, Phys. Rev. Lett. **28** (1972) 626;
P. R. Christensen, V. I. Manko, F. D. Becchetti and R. J. Nickles, Nucl. Phys. **A207** (1973) 33
8) B. M. Preedom, E. Newman and J. C. Hiebert, Phys. Rev. **166** (1968) 1156
9) M. R. Cates, J. B. Ball and E. Newman, Phys. Rev. **187** (1969) 1682
10) A. Saha, G. D. Jones, L. W. Put and R. H. Siemssen, Phys. Lett. **82B** (1979) 208
11) D. Kurath and I. S. Towner, Nucl. Phys. **A222** (1974) 1
12) R. S. Tickle, W. S. Gray and R. D. Bent, Phys. Lett. **92B** (1980) 283
13) J. R. Erskine, T. H. Braid and J. C. Stoltzfus, Nucl. Instr. **135** (1976) 76
14) D. Shapira, R. M. DeVries, H. W. Fulbright, J. Toke and M. R. Clover, Nucl. Instr. **129** (1975) 123
15) C. J. Borkowski and M. K. Kopp, Rev. Sci. Instr. **39** (1968) 1515
16) J. B. Ball, R. L. Auble and P. G. Roos, Phys. Rev. **C4** (1971) 196
17) J. B. Ball, R. L. Auble and P. G. Roos, Phys. Lett. **29B** (1969) 172
18) F. D. Becchetti, J. Jänecke and D. Overway, to be published
19) P. D. Kunz, Program DWUCK5, unpublished
20) P. Schwandt *et al.*, Indiana Univ. Cyclotron Facility Progress Report (1978) p. 93
21) K. S. Toth, J. L. C. Ford, G. R. Satchler, E. E. Gross, D. C. Hensley, S. T. Thornton and T. C. Schweizer, Phys. Rev. **C14** (1976) 1471
22) O. Lkhagva and I. Rotter, Yad. Fiz. **11** (1970) 1037; Sov. J. Nucl. Phys. **11** (1971) 225
23) D. Kurath, Comments on Nucl. and Part. Phys. **5** (1972) 55
24) J. P. Elliott, J. Hope and H. A. Jahn, Phil. Trans. **A246** (1953) 241
25) E. R. Flynn, J. G. Beery and A. G. Blair, Nucl. Phys. **A218** (1974) 285
26) D. H. Feng, M. A. Nagarajan, M. R. Strayer, M. Vallieres and W. T. Pinkston, Phys. Rev. Lett. **44** (1980) 1037
27) W. P. Alford, R. E. Anderson, P. A. Batay-Csorba, D. A. Lind, H. H. Wieman and C. D. Zafiratos, Nucl. Phys. **A293** (1977) 83
28) W. P. Alford, R. E. Anderson, P. A. Batay-Csorba, R. A. Emigh, D. A. Lind, P. A. Smith and C. D. Zafiratos, Nucl. Phys. **A330** (1979) 77
29) R. S. Tickle, W. S. Gray and R. D. Bent, Indiana Univ. Cyclotron Facility Progress Report (1979) p. 100
30) R. Maier, G. Korshinek, P. Spolaore, W. Kutschera, H. J. Maier and W. Goldstein, Nucl. Instr. **155** (1978) 55
31) F. D. Becchetti, K. T. Hecht, J. Jänecke and D. Overway, Nucl. Phys. **A339** (1980) 132